

Photophysical properties of porphyrin derivatives: Influence of the alkyl chains in homogeneous and micro-heterogeneous systems

Sandra Cruz dos Santos^a, Leonardo Marmo Moreira^b, Diogo La Rosa Novo^a,
Luiza Rosimeri Romano Santin^a, Daniela Bianchini^a, Juliano Alves Bonacin^c,
Ana Paula Romani^d, Adjaci Uchoa Fernandes^e, Maurício S. Baptista^f
and Hueder Paulo Moisés de Oliveira^{*g}

^aCentro de Ciências Químicas, Farmacêuticas e de Alimentos, Universidade Federal de Pelotas (UFPEL), Campus Universitário S/N, 96160-000 Capão do Leão-RS, Brazil

^bDepartamento de Zootecnia (DEZOO), Universidade Federal de São João Del Rei (UFSJ), 36301-360 São João Del Rei-MG, Brazil

^cInstituto de Química, Universidade de Campinas, UNICAMP, P.O. Box 6154, 13083-970 Campinas-SP, Brazil

^dCentro de Engenharia, Modelagem e Ciências Sociais Aplicadas, Universidade Federal do ABC (UFABC), Avenida dos Estados 5001, Bairro Bangu, 09210-170 Santo André-SP, Brazil

^eUniversidade Camilo Castelo Branco, São José dos Campos-SP, Brazil

^fInstituto de Química by Instituto de Química, Universidade de São Paulo USP, São Paulo-SP, Brazil

^gCentro de Ciências Naturais e Humanas, Universidade Federal do ABC (UFABC), Avenida dos Estados 5001, Bairro Santa Terezinha, 09210-580 Santo André-SP, Brazil

Received 16 September 2014

Accepted 16 March 2015

ABSTRACT: This work is focused on the evaluation of the photophysical properties of protoporphyrin-IX derivatives with different alkyl chains. The goal of this work is to understand the physicochemical properties and select prototypes of photosensitizers for photodynamic therapy. Solvents with different dielectric constants were used to obtain relevant data on different physical and chemical processes, such as fluorescence quantum yield and emission level of aggregation in nonpolar media. In addition, studies were conducted in micro-heterogeneous systems through the interaction of porphyrin derivatives with different surfactants, such as cetyltrimethylammonium bromide, sodium dodecyl sulfate and octyl phenol ethoxylate. The compounds were characterized by electronic absorption spectroscopy in the ultraviolet-visible region and fluorescence emission spectroscopy. The comparative study between the different chemical environments evaluated in the present study represents a relevant contribution to the comprehension of the properties acquired by the porphyrins in different micro-heterogeneous systems, which allows us to understand various interactions that these compounds are subject in biological medium, such as the influence of the polarity of the medium in the reactivity of porphyrins with nonpolar substituents. These results show the decisive physicochemical influence of the alkyl chains on the properties of the tetraazomacrocyclic porphyrin.

KEYWORDS: protoporphyrin-IX, fluorescence, solvatochromism, photodynamic therapy (PDT), solvent effects, micellar systems.

INTRODUCTION

Photosensitizers (PS) are compounds that play a vital role in photodynamic therapy (PDT). Activation of PS

*Correspondence to: Hueder Paulo Moisés de Oliveira, email: hueder.paulo@ufabc.edu.br, +55 11-4996-0155

using a radiation of appropriate wavelength is applied for treating diseases characterized by uncontrolled cell growth, such as cancer, and various types of microbial infections including diseases caused by bacteria, fungi and protozoa [1, 2].

Porphyrins and their derivatives, due to their interesting photophysical, photochemical and electrochemical properties [3, 4], as well as their ability to be accumulated in tissues of rapid growth as the tumor tissue [5, 6], in recent years have aroused great interest as drugs in PDT [7–12]. A typical example is the Photophrin[®], a commercial PS consisting basically of porphyrin derivatives, whose use is approved by the FDA, the regulatory authority in the United States [13, 14].

However, a drawback concerning the applications of porphyrins in biological environment is the formation of aggregates in aqueous media, due to π - π^* interactions and the hydrophobicity of these compounds [7, 15]. This feature affects the ability of porphyrins to be used as photoactive principle in PS biologically friendly [16]. To minimize this problem, many groups have studied the association of porphyrins with models of micellar systems, polymeric nanoparticles, dendrimers and liposomes [7, 17, 18], in order to investigate the interactions between photosensitizers and potential carriers of drugs, since the aforementioned micro-heterogeneous systems can mimic biological systems, *e.g.* plasma membranes and biological tissues [19, 20]. The transport of porphyrins in biological medium through micro-heterogeneous systems has been considered an interesting alternative to enabling the delivery of the PS [7, 18]. Thus, it is necessary to evaluate prototypes of the associations of porphyrin-micro-heterogeneous systems before developing efficient tests *in vivo*, so that the most suitable candidates to a set of tests on animals can be known beforehand.

Moreover, such studies allow the acquisition of physicochemical information, which is prerequisites to obtain an adequate interpretation regarding the results in a biological environment, *i.e.* to an effective understanding of biological-chemical action that the porphyrin micro-heterogeneous system may produce in a biological environment.

In this sense this work is focused on the influence of the hydrophobic alkyl chains, which were obtained by the esterification of propionic acid groups of the protoporphyrin-IX (Pp-IX), in homogeneous systems (polar and nonpolar solvents, donors or receptors of hydrogen bonds) and micellar structures (consisting of active agents on surfaces, *i.e.* “surfactants”) in the photophysical properties of these compounds in order to provide a model for drug carrier systems.

The goal of generate several derivatives of Pp-IX is understand the structure-activity relationships and find new candidates for PDT. It should be mentioned that porphyrins have a well-established photodynamic. Spectroscopic and photophysical properties of the porphyrins were investigated in detail in a significant

number of organic solvents as well as in the presence of surfactants using techniques of steady state, such as electronic absorption spectroscopy in ultraviolet-visible (UV-vis) region and fluorescence emission spectroscopy. The study of the phenomena involved in the excited state is a key step to understand the photophysical behavior of these compounds as a function of different porphyrin-surfactant interactions. Therefore, studies were conducted in micro-heterogeneous systems through the interaction of porphyrin derivatives with different surfactants, such as cetyltrimethylammonium bromide (CTAB, cationic surfactant), sodium dodecyl sulfate (SDS, anionic surfactant) and octyl phenol ethoxylate (Triton X-100, non-ionic surfactant). The instrumental analyzes associated with measurements of fluorescence lifetimes have contributed to understand the mechanisms of photophysical emission of each porphyrin derivative.

RESULTS AND DISCUSSION

Spectroscopic studies of porphyrins in homogeneous systems

Studies of the influence of solvent on the spectroscopic properties of porphyrins were conducted in this work. Changes in absorption intensity as a function of the solvent and the type of porphyrin can be observed in the electronic absorption spectra, which are shown in Fig. 1. The band of higher absorptivity observed around 405 nm is denominated Soret band or B⁰⁻⁰ band. Four other bands, which are known as Q-bands (Q_x; Q_y), can be observed in the electronic spectra of porphyrins in regions of lower energies. Both the Soret band and the Q-bands are transitions of π - π^* type [21, 22]. The Q-bands are situated between 480 and 700 nm, being related to transitions from the ground state to vibrational levels (Q_x^{0,0}, Q_x^{0,1}) and (Q_y^{0,0}, Q_y^{0,1}) of excited state S1 [23]. Although the intensities of the Q-bands are 10 to 20 times smaller than the Soret band, the majority of clinical studies on PDT require the use of spectral regions around 630 nm, which is known as “therapeutic window.” This occurs due to a great penetration of light into tissues by the longer wavelengths, which means that this absorption band has greater efficiency in treatments by photodynamic therapy, since a larger portion of the dye can be excited [24]. The “therapeutic window” is explained by the presence of endogenous dyes in different biological tissues, which compete with PS by the photons emitted by the source. In fact, two of the most important biological dyes are heme moieties of hemoproteins and the melanin, being the last one responsible for the characteristic pigmentation of the human epidermis. Both biological dyes have significant absorption in the same spectral range where porphyrin dyes have the greater absorption, in other words, around 400 nm (Soret band).

The emission spectra of fluorescence of the porphyrins in ACN, EtOH and DMSO are shown in Figs. 1b, 1d

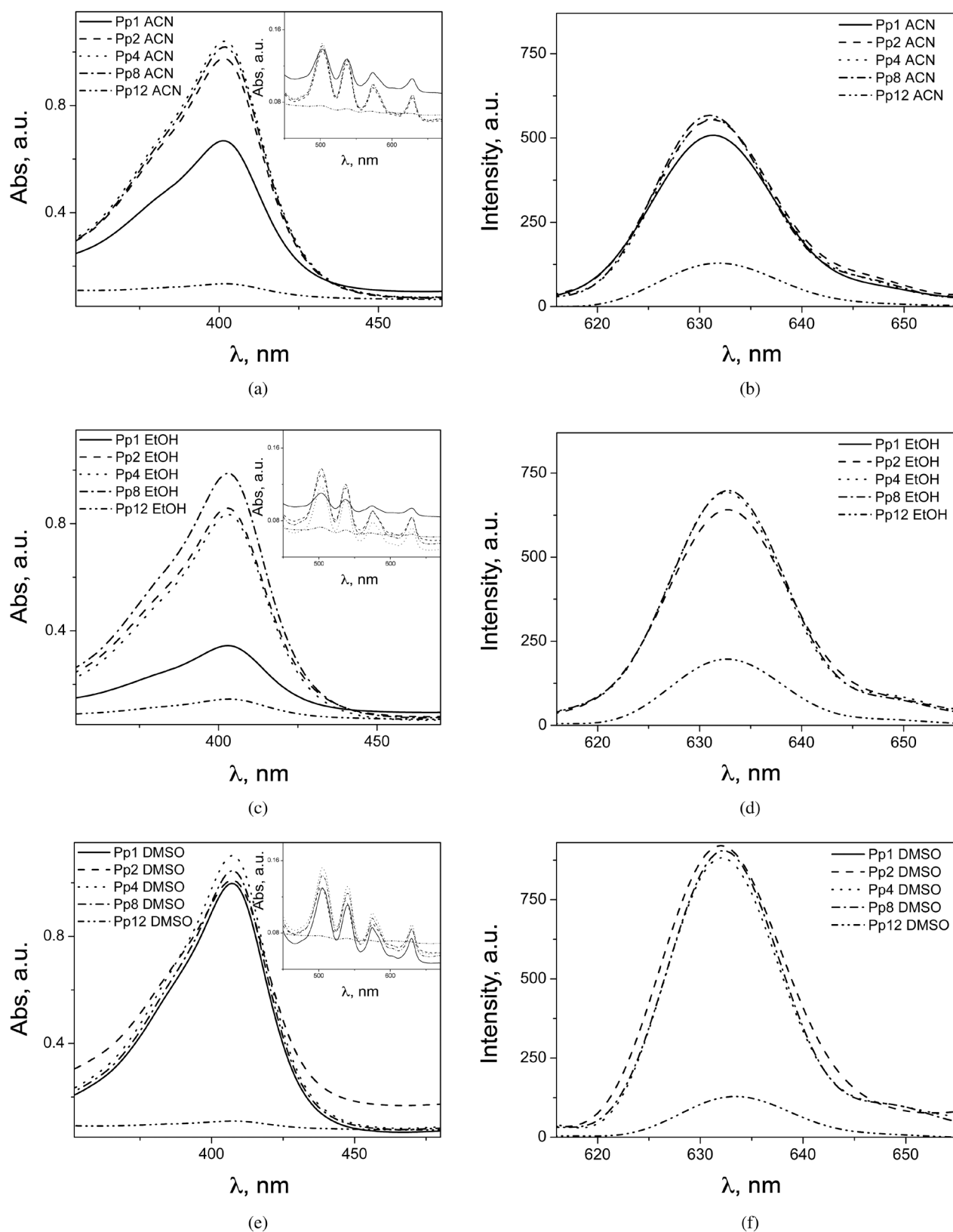


Fig. 1. Electronic absorption spectra in the UV-vis region to the porphyrins dissolved in different organic solvents: (a) ACN, (c) EtOH, (e) DMSO; Fluorescence emission spectra of the porphyrins in different organic solvents: (b) ACN, (d) EtOH, (f) DMSO. $\lambda_{\text{exc}} = \lambda_{\text{maxAbs}}$. Molar concentration: 5.0×10^{-6} M. The insets show the expanded region of Q-bands in the UV-vis spectra to the porphyrins dissolved in different organic solvents

and 1f, respectively. In these spectra, an emission band with relatively high intensity is observed near 630 nm. Significant difference is observed in the spectral shapes, which indicates that the solvent has influence on the energy level of the orbitals involved in electronic transitions $\pi \rightarrow \pi^*$.

The solvatochromism observed in this study was evaluated through the solvent parameters shown in Table 1 — scale $E_T(30)$, dipole moment (μ), dielectric constant (ϵ), absolute viscosity (η) and refractive index (n) — in order of increasing polarity.

The absorption and emission wavelength are strongly dependent on the structure and solvent. For example, Fig. 2 shows the normalized intensities of absorption and emission of Pp12 in different solvents. In this case the absorption wavelengths (at the maximum intensity — λ_A) show a displacement in the following order: DMSO > THF = DMF > EtOH > MeOH = ACN. On the other hand, the emission wavelengths (at the maximum intensity — λ_F) is THF > EtOH > DMF > DMSO = MeOH > ACN. Based on these results, an order of maximum intensity for the Soret band, according to the

solvent, can be constructed: THF > DMF > DMSO > ACN > EtOH > MeOH. A significant interference in electronic absorption of compounds is observed through a bathochromic effect of the bands in the spectral range between 400 and 407 nm, according to the polarity of the solvent. The different solvents studied have shown a bathochromic effect (positive) as the polarity decreases. Thus, the bathochromic effect of the compounds is higher in non-protic solvents, which indicates rearrangement of the charge of solute molecules under excitation electronics [27]. An identical spectral behavior was observed for the other porphyrin derivatives. In most cases, the bands are shifted to shorter wavelengths as the solvent polarity is increased, indicating a partial reduction of aggregate formation of type J or H [28].

The band intensity (intensity of absorbed light) of the Pp12 is more affected than other porphyrin derivatives by the change of solvent. In addition, the intensity of absorbance of Pp12 in all studied solvents is very low when compared to other porphyrin derivatives. This could be explained by the great influence of the nonpolar chains inserted into the porphyrin, which would reduce

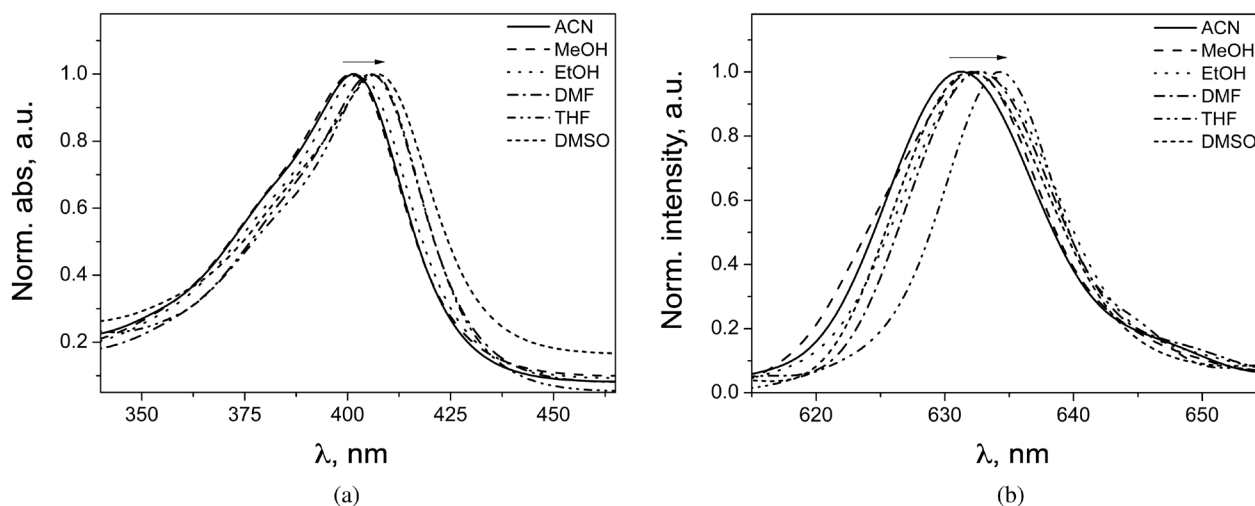


Fig. 2. Spectra of Pp12 with normalized intensities, obtained in different organic solvents (5.0×10^{-6} M): (a) absorption spectra of UV-vis, (b) emission spectra of fluorescence

Table 1. Physicochemical parameters of the solvents

Solvent	$E_T(30)$ (kcal/mol) [25]	μ (Debye) [26]	ϵ [26]	η (cP) [26]	n [26]
MeOH	55.4	1.7	32.6	0.6	1.326
EtOH	51.9	1.7	22.4	1.08	1.359
ACN	45.6	3.2	37.5	0.38	1.342
DMSO	45.1	3.96	46.6	2.0	1.476
DMF	43.2	3.8	36.7	0.82	1.427
THF	37.4	1.75	7.6	0.55	1.404

$E_T(30)$ = solvent polarity (25 °C); μ = dipole moment; ϵ = dielectric constant (20 °C); η = absolute viscosity (25 °C); n = refractive index (25 °C).

its affinity for solvents with higher polarity. The intensity of fluorescence emission of Pp12 is relatively low when compared to other porphyrin derivatives, which indicates that this porphyrin derivative is not the best alternative to be tested as a prototype of photosensitizer in PDT. Furthermore, it should be considered an additional factor that decreases the potential use of this compound as PS. The long hydrophobic alkyl chains of Pp12 confer the lowest polarity among porphyrin derivatives, which reduces its solubility in polar solvents, such as water. This low solubility favors the aggregation and decreases the quantum yield of emission.

Table 2 shows the results of the maximum absorption wavelength (λ_A), molar absorptivity coefficient (ϵ), maximum emission wavelength (λ_F), Stokes shift ($\nu_A - \nu_F$), fluorescence quantum yield based on the absorptivity of the anthracene (Φ_F), fluorescence lifetime ($\lambda_{exc} = 414$ nm and $\lambda_{ems} = 630$ nm) (τ), constant of radiative decay (fluorescence decay, K_r) and constant of non-radiative decay (K_{nr}). K_r and K_{nr} were calculated from Equations 1 and 2, respectively.

In this study, we have also calculated the constants of fluorescence decay and non-radiative decay from theoretical data. The oscillator strength is an important parameter to be evaluated for fluorescent compounds and corresponds to the effective number of the electrons that are promoted from ground to excited state. These transitions give the absorption area in the electronic spectrum [29]. E_{s1} corresponds to the energy of the singlet state S_1 , which is calculated according to Equation 3. This is defined as the intersection between the normalized spectra of absorption and fluorescence with the oscillator strength (f), which is calculated from Equation 4. In this equation, n is the refractive index of the solvent, $\Delta\nu_{1/2}$ is the full width at half maximum of the absorption band and ϵ is the molar absorptivity coefficient. The natural radiative lifetime of the excited singlet state is represented by τ_0 , which is shown in Fig. 3. The parameter $\tilde{\nu}_{max}$ is the frequency of maximum absorption and f is the oscillator strength, which is calculated from Equation 4. The calculated fluorescence lifetime (τ_{F-calc}) is obtained from τ_0 and Φ_F , according to Equation 6.

The calculated constant of fluorescence decay of singlet state (K_{r-calc}) was obtained from Equation 7. The calculated constant of non-radiative decay ($K_{nr-calc}$) was obtained from Equation 8.

$$K_r = \Phi_F / \tau \quad (1)$$

$$K_{nr} = (1 - \Phi_F) / \tau \quad (2)$$

$$E_{s1} = 11.96 \times 10^4 / [(\lambda_A + \lambda_F) / 2] \quad (3)$$

$$f = 4.32 \times 10^{-9} \Delta\nu_{1/2} \epsilon_{max} / n \quad (4)$$

$$\tau_0 = 1.5 / (\tilde{\nu}_{max}^2 f) \quad (5)$$

$$\tau_{F-calc} = \tau_0 \Phi_F \quad (6)$$

$$K_{r-calc} = \Phi_F / (\tau_{F-calc}) \quad (7)$$

$$K_{nr-calc} = 1 - \Phi_F / (\tau_{F-calc}) \quad (8)$$

Based on the values of maximum wavelength of absorption and emission (Table 2), an hypsochromic shift is observed as the solvent polarity is increased. The parameter Φ_F shows higher values in less polar solvents, as observed to DMSO, DMF and THF. On the other hand, Φ_F has lower values in solvents with higher polarity, as EtOH, MeOH and ACN. The Stokes shift indicates the red shift of the maximum fluorescence wavelength in relation to the maximum absorption wavelength. Table 2 shows lower values of $\nu_A - \nu_F$ as the solvent polarity is decreased. This indicates a higher extension of interactions of porphyrin derivatives with polar solvents. Considering the bands of transitions $\pi - \pi^*$ for monomeric units of porphyrin, which corresponds to porphyrin not aggregated each other, the increasing dielectric constant tends to shift the porphyrin spectrum to red (bathochromic shift), since the orbitals π^* are more polarizable and accessible than orbitals π involved in electronic transitions.

The hydrophobic chain length inserted in the porphyrins has a great influence in the spectral behavior, specially for the porphyrin derivative containing dodecyl groups (Pp12). As the carbon chain increases, the polarity of porphyrin derivatives decreases. Thus, the aggregate formation is reduced due to the increased solubility of porphyrin in less polar solvents. This can be evidenced by the higher Φ_F values for Pp12 in DMF and THF compared with polar solvents, whose Φ_F is close to zero.

In order to understand the characteristic mechanisms of emission for each type of porphyrin, the fluorescence decays were studied in different solvents: DMSO, EtOH and ACN. Fig. 3 shows the decay profiles of Pp2 and Pp12 for these solvents.

Considering measurements obtained in the same medium, the profiles of the fluorescence decay for porphyrin derivatives are very similar. It should be considered that the length of the alkyl chain is not a significant parameter. The results show a simple exponential decay for all systems suggesting only one fluorescent specie. The parameters obtained from the fluorescence decay adjusted by a monoexponential curve are shown in Table 2. It should be noticed that in all solvents, the fluorescence decay parameters depend on the molecular structure of the solvent, with special emphasis on its polarity. In addition, it is well-known that both the values of fluorescence lifetime and the fluorescence quantum yield have a decreasing tendency as the solvent polarity increases [30, 31].

The viscosity is another important parameter since the fluorescence lifetime depends on the viscosity and dielectric constant of the solvent. The influence of the viscosity in the rotational lifetime was evaluated in polar and nonpolar solvents and was verified a linear relationship between the rotational relaxation times and the solvent viscosity [32, 33]. This dependence indicates that the deactivation process of the excited state in solution becomes slower in more viscous media [32, 33].

Table 2. Photophysical properties of the porphyrin derivatives

Solvent	λ_A , nm	ϵ , M ⁻¹ cm ⁻¹	λ_F , nm	$\nu_A - \nu_F$, cm ⁻¹	Φ_F	τ , ns	K_r , 10 ⁷ s ⁻¹	K_{nr} , 10 ⁷ s ⁻¹	E_{s1}	f	τ_0 , ns	T_{F-calc} , ns	K_{r-calc} , 10 ⁷ s ⁻¹	$K_{nr-calc}$, 10 ⁷ s ⁻¹
<i>Pp1</i>														
MeOH	401	70 180	632	9114.87	0.10	—	—	—	231.56	0.96	2.50	0.25	39.96	359.65
EtOH	403	68 956	633	9016.11	0.12	12.33	0.97	7.14	230.89	0.83	2.93	0.35	34.18	250.68
ACN	401	137 666	631	9089.80	0.16	7.07	2.26	11.88	231.78	1.42	1.69	0.27	59.02	309.83
DMSO	407	199 536	632	8747.24	0.43	17.57	0.43	2.45	230.22	1.56	1.60	0.69	62.65	83.051
DMF	406	231 346	632.5	8820.27	0.39	—	—	—	230.33	1.94	1.27	0.50	78.46	122.71
THF	406	240 920	634.5	8870.10	0.32	—	—	—	229.89	2.39	1.03	0.33	96.75	205.60
<i>Pp2</i>														
MeOH	401	133 880	632	9114.87	0.17	—	—	—	231.56	1.27	1.89	0.19	52.80	475.17
EtOH	403	171 644	633	9016.11	0.20	12.68	1.58	6.31	230.89	1.57	1.55	0.19	64.56	473.40
ACN	401	195 100	631	9089.80	0.17	7.16	2.37	11.59	231.78	1.83	1.32	0.21	75.80	397.97
DMSO	407	201 870	632	8747.24	0.45	17.41	0.45	2.58	230.22	1.85	1.34	0.58	74.50	98.75
DMF	406	223 730	632.5	8820.27	0.40	—	—	—	230.33	1.90	1.30	0.51	77.04	120.50
THF	406	242 000	634.5	8870.10	0.32	—	—	—	229.89	2.06	1.20	0.39	83.20	176.79
<i>Pp4</i>														
MeOH	401	147 900	632	9114.87	0.17	—	—	—	231.56	1.41	1.71	0.17	58.48	526.31
EtOH	403	167 002	633	9016.11	0.20	12.65	1.58	6.32	230.89	1.48	1.65	0.20	60.58	444.24
ACN	401	208 020	631	9089.80	0.17	6.96	2.44	11.93	231.78	1.93	1.25	0.20	79.96	419.80
DMSO	407	220 224	632	8747.24	0.40	17.78	0.4	2.24	230.22	1.73	1.44	0.62	69.64	92.31
DMF	406	223 164	632.5	8820.27	0.41	—	—	—	230.33	1.86	1.33	0.52	75.27	117.73
THF	406	216 520	634.5	8870.10	0.33	—	—	—	229.89	1.85	1.34	0.43	74.90	159.17
<i>Pp8</i>														
MeOH	401	160 460	632	9114.87	0.18	—	—	—	231.56	1.49	1.62	0.16	61.63	554.69
EtOH	403	197 670	633	9016.11	0.21	12.65	1.66	6.24	230.89	1.75	1.39	0.17	71.70	525.82
ACN	401	203 660	631	9089.80	0.17	6.92	2.46	11.99	231.78	1.76	1.37	0.22	72.85	382.48
DMSO	407	208 926	632	8747.24	0.41	17.6	0.41	2.33	230.22	1.70	1.46	0.63	68.42	90.70
DMF	406	220 428	632.5	8820.27	0.40	—	—	—	230.33	1.85	1.33	0.52	75.02	117.34
THF	406	242 860	634.5	8870.10	0.34	—	—	—	229.89	2.04	1.21	0.39	82.42	175.14
<i>Pp12</i>														
MeOH	401	17 800	632	9114.87	0.01	—	—	—	231.56	0.14	1.74	1.74	5.74	51.62
EtOH	403	29 070	633	9016.11	0.05	12.47	0.4	7.61	230.89	0.71	3.45	0.41	29.02	212.83
ACN	401	26 880	631	9089.80	0.04	7.08	0.56	13.56	231.78	0.25	9.63	1.54	10.39	54.53
DMSO	407	22 068	632	8747.24	0.05	16.45	0.05	0.3	230.22	0.23	1.06	4.56	9.43	12.50
DMF	406	69 256	632.5	8820.27	0.29	—	—	—	230.33	0.76	3.25	1.27	30.75	48.09
THF	406	144 300	634.5	8870.10	0.29	—	—	—	229.89	1.27	1.94	0.62	51.49	109.42

The structures of the porphyrin derivatives are shown in Fig. 1; λ_A = maximum absorption wavelength; ϵ = molar absorptivity coefficient; λ_F = maximum emission wavelength; $(\nu_A - \nu_F)$ = Stokes shift; Φ_F = fluorescence quantum yield based on the absorptivity of the anthracene; τ = fluorescence lifetime (λ_{exc} = 414 nm and λ_{ems} = 630 nm); K_r = constant of fluorescence decay; K_{nr} = constant of non-radiative decay; E_{s1} = energy of the singlet state S_1 ; f = oscillator strength; τ_0 = natural radiative lifetime of the excited singlet state; τ_{F-calc} = calculated fluorescence lifetime; K_{r-calc} = calculated constant of fluorescence decay of the singlet state; $K_{nr-calc}$ = calculated constant of non-radiative decay.

In this work the fluorescence lifetimes are in the range of 7.0 and 17.8 ns. The lifetime in the excited state is longer for porphyrin derivatives dissolved in lower polarity solvents than those dissolved in higher polarity solvents.

According to the data presented in Table 2, the values of lifetime are in the following order: $\tau_{ACN} < \tau_{EtOH} < \tau_{DMSO}$. The viscosity of the solvents, $ACN < EtOH < DMSO$ (Table 1), corroborates the results. In addition,

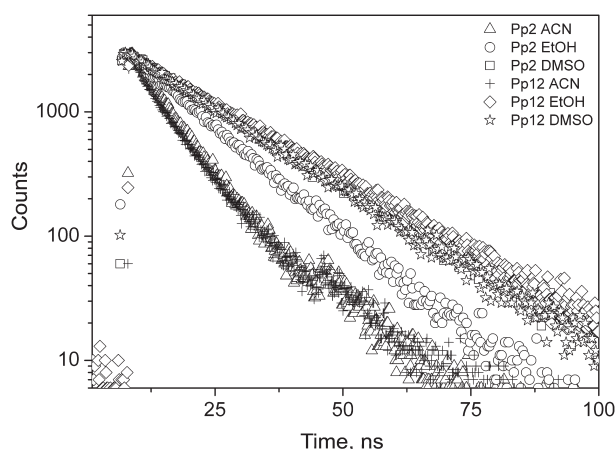


Fig. 3. Profiles of fluorescence decay for Pp2 and Pp12 dissolved in different solvents. Pulse excitation at 416 nm and emission at 630 nm

the results of $\tau_{F\text{-calc}}$ have a similar tendency observed for values obtained experimentally, with higher values in DMSO.

Other relevant results are the constants of fluorescence decay, K_r , and the constants of non-radiative decay, K_{nr} , which are shown in Table 2. K_r and K_{nr} were obtained from the fluorescence quantum yield, Φ_F , and the fluorescence lifetime, τ , according to Equations 1 and 2. It is worth mentioning that only one emitting specie or only the dominant specie was considered [34]. K_r is associated with the deactivation process of an electron π promoted from the singlet excited state (S_1) to fundamental singlet state (S_0). This process corresponds to fluorescence emission of a molecule π conjugated. K_r values increase as the alkyl chains of porphyrin derivatives increase. This behavior is related with the relaxation process of the molecules in the respective solvents. The constant K_r can be compared with that of the calculated fluorescence decay, $K_{r\text{-calc}}$, which is obtained from the absorption spectra by $1/\tau_0 \cdot K_{r\text{-calc}}$ is higher than K_r but the tendency associated to solvent polarity is the same for both. On the other hand, the K_{nr} is assigned to transitions by internal conversion and intersystem crossing. Thus, K_{nr} is a constant for non-radiative decay due to electron transfer (ET) from negative charge to positive one. This process is related to an intramolecular electronic transfer from S_1 to S_0 [35]. These results suggest that the relation between K_r and K_{nr} depends on the π extension of the S_1 excited state of the molecule with the solvent.

It should be mentioned that the quantum yields in polar solvents are lower than those observed in solvents with lower polarity. In Table 2, the porphyrin derivatives show that K_r is higher than K_{nr} . This occurs due the affinity of the porphyrin derivatives for less polar solvents, where the appropriated micro-polarity and the viscosity suppress the non-radiative processes. Thus, the fluorescence quantum yield and K_r are larger.

Spectroscopic studies of porphyrins derivatives in micro-heterogeneous systems: micelles

Porphyrins often form aggregates in aqueous medium, being necessary its dispersion in micro-heterogeneous systems in order to be employed in PDT. The best relation porphyrin/surfactant should be known for this use. Figs. 4 and 5 show the absorption and emission spectra, respectively, obtained for porphyrin derivatives in different micro-heterogeneous systems, where the micellar structures prevail.

The maximum absorption wavelength in the presence of neutral micelles (Triton X-100, Fig. 4a) can be compared to the wavelength obtained in homogeneous systems with less polarity ($\lambda_{\text{abs}} \sim 408$ nm), independently of the pH analyzed. The results demonstrate the affinity of porphyrin derivatives for non-ionic surfactants. This type of surfactant tends to favor the interaction with nonpolar porphyrins.

The absorption spectra suggest a better interaction of the porphyrin derivatives with the cationic surfactant (Fig. 4c) than with the anionic surfactant (Fig. 4b). This can be evidenced through the Soret bands, which are better defined in the cationic micelles. The displacement observed for the wavelengths can be attributed to the different forms of interaction of porphyrin derivatives with the surfactants [36].

In this context, it should be emphasized two fundamental contributions of the porphyrin-surfactant interactions: the nonpolar interactions between the porphyrin derivative and the nonpolar chain of the surfactants, and the polar interactions between the porphyrin derivative and the polar head of the surfactants. The former type of interaction should have an important role considering the nonpolar characteristics of the porphyrin derivatives that are being studied. In the latter, the cationic surfactant has greater interaction with the porphyrin rings than the anionic surfactant. This occurs due the interaction of the cationic moiety of the surfactant CTAB with the pyrrolic nitrogens of the porphyrin ring. Indeed, the polar head of the surfactant CTAB acts as an acid coordination center (Lewis acid) for the lone electrons pair from pyrrolic nitrogens of the tetraazomacrocycle of the porphyrin (Lewis base).

Fig. 4 also shows a great dependence of the spectral properties with the pH in micellar systems. The spectra obtained in anionic micelles (SDS), except the spectrum obtained at pH 2.0, show a splitting of the Soret band. In these spectra, the Soret band exhibits components which are shifted to blue wavenumber and other components which are shifted to red wavenumber when compared to the monomeric form in non-ionic micelles. This indicates the presence of different intermolecular interactions and conformation of porphyrins, probably due to the formation of aggregates. These results are according to those reported by Inamura *et al.* [37] and Scolaro *et al.* [38], which have studied the stability of the protoporphyrin-IX

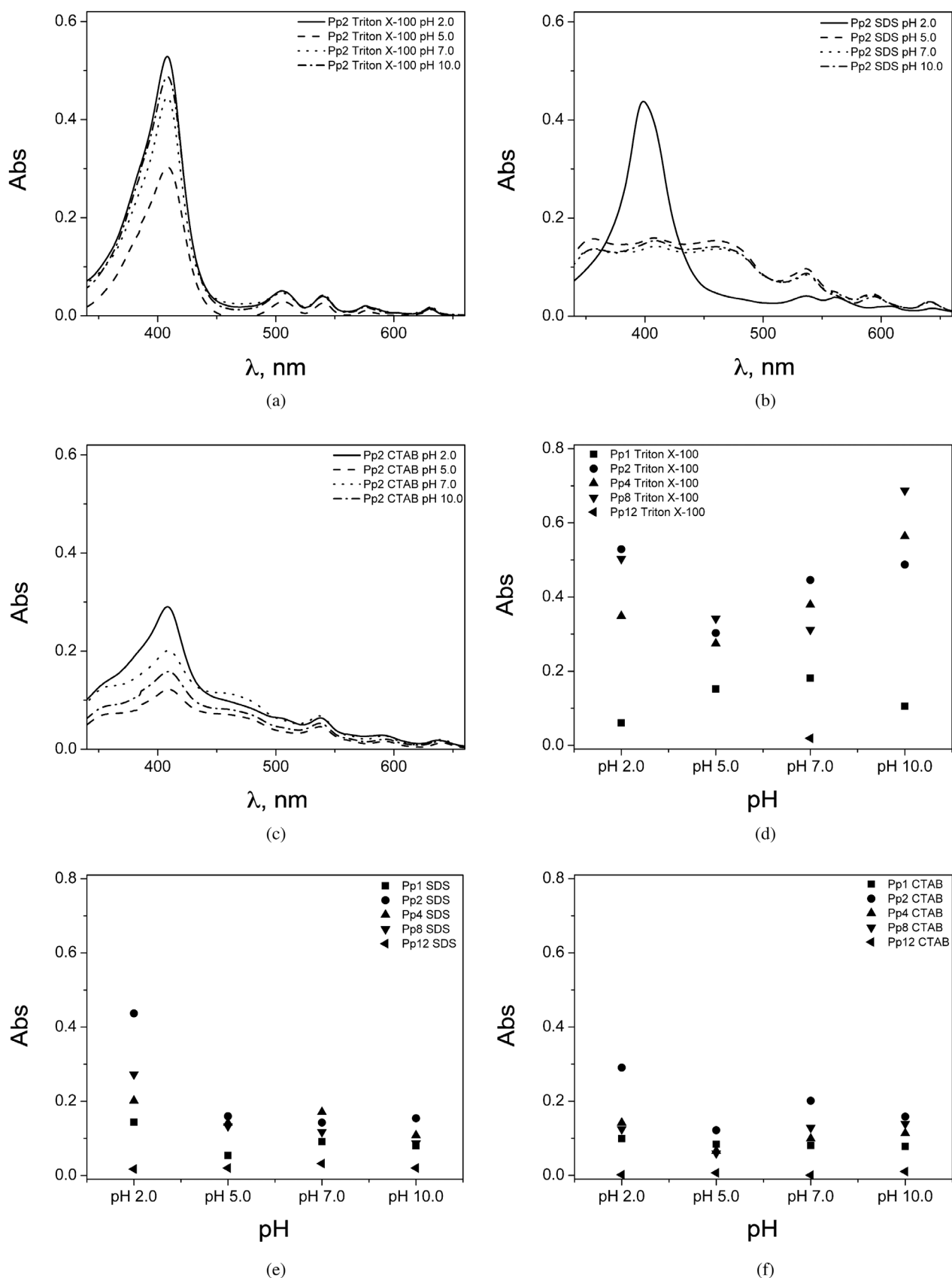


Fig. 4. Electronic absorption spectra of the UV-vis for Pp2 (5.0×10^{-6} M) in micro-heterogeneous systems: (a) Triton X-100, (b) SDS and (c) CTAB in different pH values; and maximum intensity of absorption for each porphyrin derivative (5.0×10^{-6} M): (d) Triton X-100, (e) SDS and (f) CTAB at different pH values

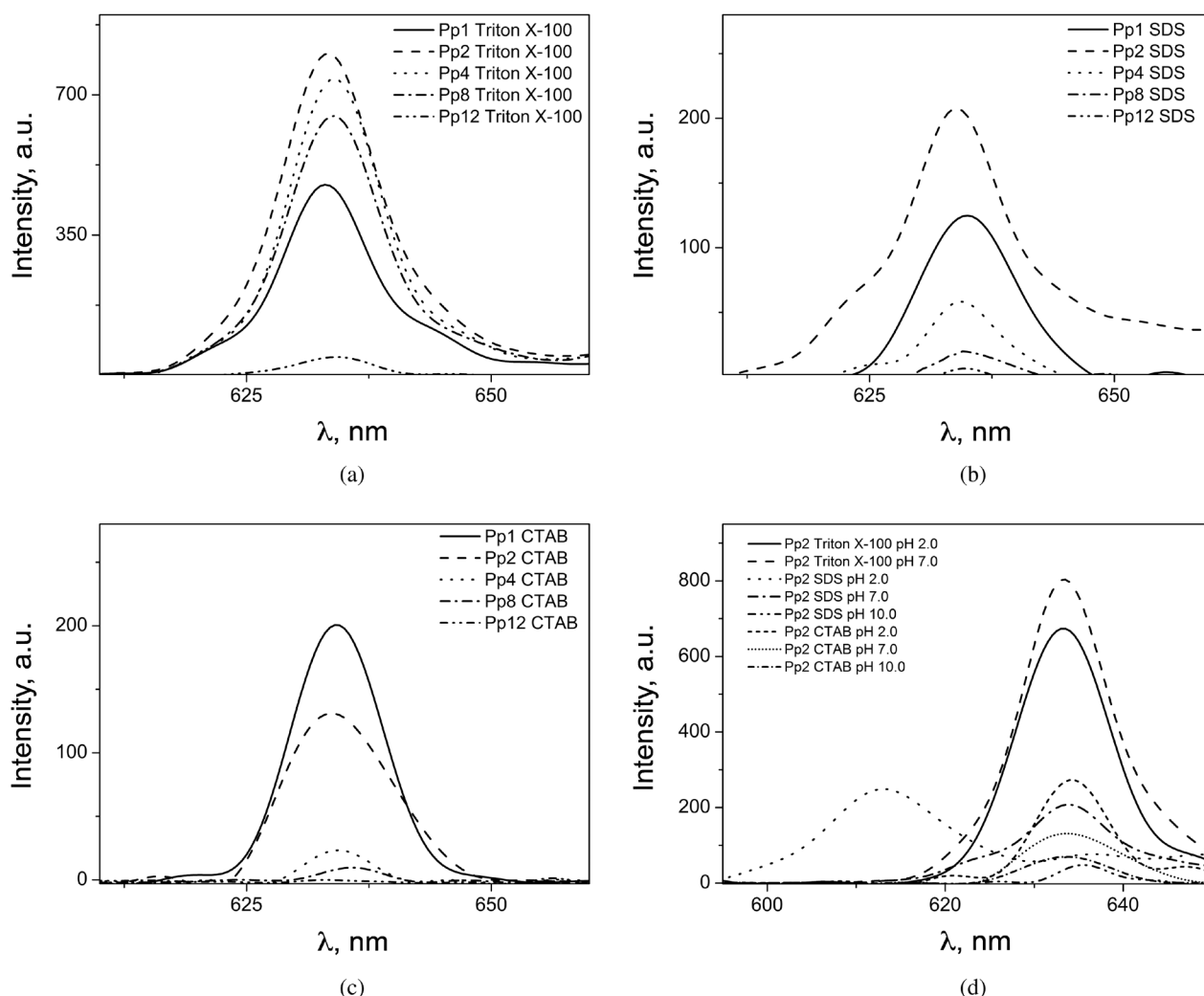


Fig. 5. Fluorescence emission spectra ($\lambda_{\text{exc}} = 408$ nm): (a) Triton X-100, (b) SDS and (c) CTAB at pH = 7.0; (d) Pp2 in Triton X-100, SDS and CTAB in different pH values. Molar concentration of porphyrin derivatives: 5.0×10^{-6} M

in aqueous solutions with different pH. The authors have observed the formation of great aggregates in moderately acidic conditions (pH = 4.8), being the aggregates identified by the splitting in the Soret band between 300 and 500 nm, as it was also observed in our studies for the anionic micelles. This behavior was explained by the formation of dimers of porphyrin, which are bonded by axial interactions of stacking π - π and by strong lateral hydrophobic "edge-to-edge." In addition, these systems can be stabilized by hydrogen bonds through side chains [36]. As seen in the literature, the monomeric form of protoporphyrin-IX is observed in the pH range between 0 and 3.0, the dimeric form is observed in pH > 8.0 and great aggregates are observed in the pH range between 3.0 and 7.0 [38].

The spectra obtained from different porphyrins in the same medium were similar but with different absorption intensities (Fig. 4). In our results, we can observe that porphyrins with longer alkyl chains have shown higher definition in the absorption spectra and an increase

in the intensity of the Soret band when compared to the protoporphyrin-IX. It indicates that the increase of nonpolar chains enhances the affinity between porphyrin and surfactant. Thus, considering the great flexibility of the porphyrin ring, especially in the free bases form, the extension of Van der Waals interactions are representative, which favor the stabilization by nonpolar interactions. This suggests that probably the hydrophobic interaction between the nonpolar chain of the ionic surfactant and the porphyrin is the main type of supramolecular contact. This monomeric form observed in more acidic media is associated to the efficient protonation of pyrrolic nitrogens, which are inside the porphyrin ring [37]. In our study, it was also observed a better solubility of the monomeric form of protoporphyrin-IX derivatives by anionic micelles with higher acidity.

The emission spectra of the five compounds, with exception of SDS micelles at pH 2.0, exhibit relatively high intensity band between 620 and 660 nm. The maximum emission wavelength was changed according

to the type of surfactant used or the size of the porphyrin derivative chains. In these media, λ_F values were close to those obtained in THF, which confirms that the emitting species in micelles are located in less polar environment. In ionic surfactants medium, a large suppression of fluorescence was observed, especially in CTAB micelles, where increasing alkyl chain has direct influence in the increase of fluorescence suppression. However, this suppression was not very efficient at pH 2.0. Another interesting result was the displacement of the band to shorter wavelengths in the anionic media at pH 2.0.

The fluorescence quantum yields (Table 3) were calculated for each solution in order to obtain an indication of efficiency of fluorescence. Higher values of Φ_F were obtained in the neutral micelles (Triton X-100), while a large decrease was observed in cationic micelles (CTAB) for chains containing more than two carbon atoms. The chain size in the protoporphyrin-IX derivatives affects directly the values of Φ_F , being possible to observe values extremely small for the Pp12 in all micellar media.

Considering anionic micelles (SDS), the highest Φ_F value was observed for the Pp4 porphyrin derivative.

The fluorescence lifetime was also measured in micellar systems (Table 3). The excitation wavelength was 416 nm and the emission wavelength was 630 nm at 20°C. Only one fluorescence lifetime was obtained for each type of porphyrin or surfactant, suggesting the presence of only one emitting specie. Comparing porphyrins in the same micro-heterogeneous systems, where micellar structure is predominant, the lifetimes were similar. The lifetime of the micelles was observed in the following order: $\tau_{CTAB} < \tau_{SDS} < \tau_{Triton\ X-100}$. This order is in agreement with the values obtained for fluorescence quantum yields, which are dependent on the different micellar environments. These results are very close to those reported by Maiti *et al.* [39] for Pp1. The authors have assigned the increase in the lifetime of this porphyrin in micellar systems when compared to the value obtained in pure solvents (THF) and the reduction in fluorescence suppression by oxygen in micellar samples, which occurs due to the limited

Table 3. Photophysical properties of the porphyrin derivatives dispersed in micro-heterogeneous systems

Surfactant	λ_A , nm	ϵ , M ⁻¹ .cm ⁻¹	λ_F , nm	$\nu_A - \nu_F$, cm ⁻¹	Φ_F	τ , ns	τ_r , ns	K_r , 10 ⁷ s ⁻¹	K_{nr} , 10 ⁷ s ⁻¹
<i>Pp1</i>									
Triton X-100	408	36 320	663	8712.02	0.20	18.74	11.39	1.07	4.27
SDS	408	18 200	665	8761.77	0.12	16.67	2.50	0.72	5.28
CTAB	408	16 100	664	8736.93	0.18	13.95	2.34	1.29	5.88
<i>Pp2</i>									
Triton X-100	408	89 200	633.5	8724.48	0.35	18.75	13.47	1.87	3.47
SDS	409	28 520	634	8677.01	0.11	17.07	1.76	0.64	5.21
CTAB	409	40 220	633.5	8664.56	0.08	13.88	2.84	0.58	6.63
<i>Pp4</i>									
Triton X-100	408	75 840	634	8736.93	0.31	18.65	14.10	1.66	3.70
SDS	409	34 200	634.5	8689.44	0.22	16.80	2.17	1.31	4.64
CTAB	409	19 820	634.5	8689.44	0.03	14.04	3.13	0.21	6.91
<i>Pp8</i>									
Triton X-100	408	62 392	634	8736.93	0.28	18.70	13.31	1.50	3.85
SDS	409	23 440	634.5	8689.44	0.21	16.56	1.39	1.27	4.78
CTAB	410	25 700	636	8666.97	0.03	14.11	3.63	0.21	6.87
<i>Pp12</i>									
Triton X-100	412	3800	634	8498.97	0.01	18.31	14.37	0.05	5.41
SDS	406	6400	635	8882.51	0.02	16.73	1.48	0.12	5.86
CTAB	411	964	633	8533.11	0.01	13.88	4.51	0.07	7.13

The structures of the porphyrin derivatives are shown in Fig. 1; CTAB: cetyltrimethylammonium bromide; SDS: sodium dodecyl sulfate; Triton X-100: octyl phenol ethoxylate; λ_A = maximum absorption wavelength; ϵ = molar absorptivity coefficient; λ_F = maximum wavelength of the emission; $(\nu_A - \nu_F)$ = Stokes shift; Φ_F = fluorescence quantum yield based on the absorptivity of the anthracene; τ = fluorescence lifetime ($\lambda_{exc} = 414$ nm and $\lambda_{ems} = 630$ nm); τ_r = rotational correlation time; K_r = constant of fluorescence decay; K_{nr} = constant of non-radiative decay.

diffusion of this suppressor. It can be also observed an increase in the fluorescence lifetimes of the porphyrin derivatives with respect to protoporphyrin-IX.

As previously mentioned the predominant micro-heterogeneous system is the micelle. However, a significant amount of monomeric aggregates and pre-micellar aggregates of free surfactants in the solvent can be interacting with monomers or aggregates of porphyrin. This mention is relevant since the systems evaluated in this work are not trivial chemical equilibria and as well as the biological systems, suggests the coexistence of many species. It is possible that the increase in full width at half maximum of some bands, as well as some less characteristic results and even slightly differentiated from that similar studies in the literature, are related to the peculiarities of the interactions between porphyrin systems and monomeric units of surfactants as well as the pre-micellar aggregates of surfactants.

The rotational correlation times (τ_r) of the porphyrin derivatives were determined for micellar systems in order to study in more detail the formation of dimers/aggregates. This study was developed to understand the rotational movement of porphyrins, which can play a significant role in fluorescence spectroscopy. The anisotropy decay profiles of the molecules in media containing surfactants were obtained from four measurements of fluorescence decay by using crossed polarizers. The best fit of data was obtained for the decay of a monoexponential curve, which has identified a fast rotational correlation time for porphyrins in media of CTAB and SDS as well as a relatively higher rotational correlation time for Triton X-100, as shown in Table 3.

Values close to 0.1 were obtained for the static anisotropy in this study. According to Maiti *et al.* [39] the depolarization of the probe fluorescence intercalated in the micelle can be assigned to three mechanisms: (i) the rotational momentum of the probe into the micelle, (ii) the micelle rotation as a whole and (iii) the translational diffusion of the probe along the surface of the micelle. Considering the diameter of the porphyrin ring ($\sim 13 \text{ \AA}$), which is smaller than the diameter of the micelles SDS, CTAB or Triton X-100, it is possible to assume that the

porphyrin can be physically accommodated within the micelles. However, it is well-known that porphyrins are not usually in the core of the micelles, but rather in a spatial position nearest the surface [39]. Thus, the prevalence of nonpolar porphyrin derivatives studied in this work suggests that the spatial arrangement of these dyes can occur in an intermediate position between the polar heads and the micellar center.

EXPERIMENTAL

Protoporphyrin-IX and alcohols were obtained from Aldrich and Fluka, respectively. Other commercial chemicals were used without further purification. Derivatives of protoporphyrin-IX, Fig. 6, were obtained by Fischer esterification reaction, whose procedure was described previously [40, 41]. The reactions were performed at room temperature for six hours (6 h) in excess of the correspondent alcohol. After reaction time, the crude product was neutralized with ammonia solution and extracted with dichloromethane. The products were purified by column chromatography on basic alumina (Merck: Brockmann Grade V), with dichloromethane/methanol = 1000:1 (v/v), dissolved in dichloromethane and precipitated by methanol addition. All compounds were obtained with a yield exceeding 80%. The products were characterized by mass spectrometry (MicroTOF lc Bruker Daltonics, Capillary: 4000 V, Nebulizer: 0.4 bar, Dry gas rate: 5.0 L.min⁻¹, Temp: 180 °C); UV-vis spectroscopy (Shimadzu UV-2401PC spectrophotometer); ¹H NMR spectroscopy (Bruker DRX 500, 500.13 MHz, CDCl₃). Unequivocal assignments of ¹H NMR spectra were made by 2D COSY (¹H/¹H), see the figures in the Supporting information (SI).

Anal. calcd. for **Pp1 (21H,23H-Porphine-2,18-dipropionic acid, 7,12-diethenyl-3,8,13,17-tetramethyl-, 2,18-dimethyl ester)**. Yield 98%. ¹H NMR (CDCl₃, 500.13 MHz): δ , ppm -3.77 (br s, 2H, H-21 and H-23); 3.27 (t, 4H, $J = 7.5 \text{ Hz}$, H-13² and H-17²); 3.60; 3.61; 3.68 and 3.69 (4s, 14H, H-2, H-7, H-12 and H-18); 3.66 (s, 6H, 13⁴ and 17⁴); 6.18 (d, 2H, $J = 11.5 \text{ Hz}$, H-3^{2\alpha} and H-8^{2\alpha}); 6.36

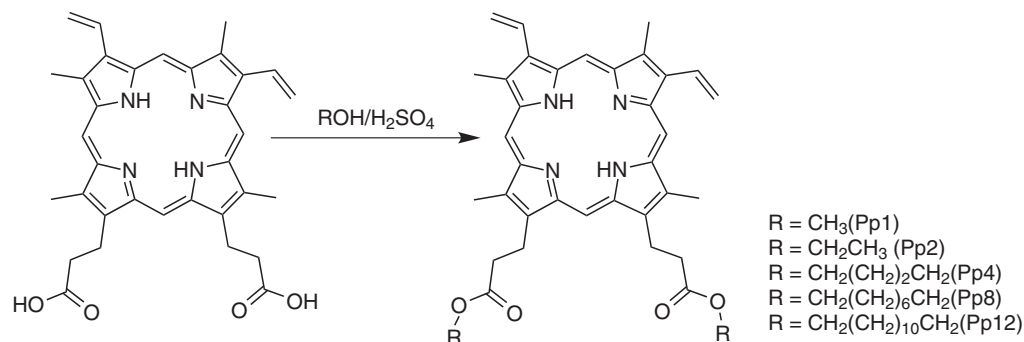


Fig. 6. Synthetic route and structural formulas of protoporphyrin-IX derivatives

(d, 2H, $J = 17.5$ Hz, H-3^{2β} and H-8^{2β}); 8.27 (dd, 2H, $J = 17.5$ and 11.5 Hz, H-3¹ and H-8¹) 10.00, 10.04, 10.14 and 10.18 (4s, 4H, H-5, H-10, H-15 and H-20). ESI-MS-TOF: m/z 591.2966 calcd. for C₃₆H₃₉N₄O₄⁺ (calcd. for [M + H]⁺ 591.2970).

Anal. calcd. for **Pp2 (21H,23H-Porphine-2,18-dipropanoic acid, 7,12-diethenyl-3,8,13,17-tetramethyl-, 2,18-diethyl ester)**. Yield 92%. ¹H NMR (CDCl₃, 500.13 MHz): δ, ppm -3.78 (br s, 2H, H-21 and H-23); 1.14 (t, 6H, $J = 7.0$ Hz, H-13⁵ and H-17⁵); 3.25 (t, 4H, $J = 7.5$ Hz, H-13² and H-17²); 3.60; 3.61; 3.67 and 3.70 (4s, 14H, H-2, H-7, H-12 and H-18); 4.14 (q, 4H, $J = 7.0$ Hz, H-13⁴ and H-17⁴); 4.38 (t, 4H, $J = 7.0$ Hz, H-13¹ and H-17¹); 6.18 (d, 2H, $J = 11.5$ Hz, H-3^{2α} and H-8^{2α}); 6.36 (d, 2H, $J = 18.0$ Hz, H-3^{2β} and H-8^{2β}); 8.26 (m, 2H, H-3¹ and H-8¹); 10.01, 10.03, 10.12 and 10.16 (4s, 4H, H-5, H-10, H-15 and H-20). ESI-MS-TOF: m/z 619.3279 calcd. for C₃₈H₄₃N₄O₄⁺ (calcd. for [M + H]⁺ 619.3275).

Anal. calcd. for **Pp4 (21H,23H-Porphine-2,18-dipropanoic acid, 7,12-diethenyl-3,8,13,17-tetramethyl-, 2,18-dibutyl ester)**. Yield 96%. ¹H NMR (CDCl₃, 300 MHz): δ, ppm -3.69 (br s, 2H, H-21 and H-23); 0.711 (t, 6H, $J = 7.5$ Hz, H-13⁷ and H-17⁷); 1.14–1.21 (m, 4H, H-13⁶ and H-17⁶); 1.42–1.51 (m, 4H, H-13⁵ and H-17⁵); 3.23 (t, 4H, $J = 7.5$ Hz, H-13² and H-17²); 3.56 (6H); 3.60 (3H) and 3.62 (3H) (3s, 12H, H-2, H-7, H-12 and H-18); 4.07 (t, 4H, $J = 7.0$ Hz, H-13⁴ and H-17⁴); 4.36 (t, 4H, $J = 7.0$ Hz, H-13¹ and H-17¹); 6.15 (two overlapping dd, 2H, $J = 11.5$ and $J = 2.0$ Hz, H-3^{2α} and H-8^{2α}); 6.30 (two overlapping dd, 2H, $J = 18.0$ Hz, H-3^{2β} and H-8^{2β}); 8.16 and 8.22 (two dd, 2H, $J = 17.5$ and 11.5 Hz, H-3¹ and H-8¹) 9.91, 9.94 and 10.03 (4s, 4H, H-5, H-10, H-15 and H-20). ESI-MS-TOF: m/z 675.3905 calcd. for C₄₂H₅₁N₄O₄⁺ (calcd. for [M + H]⁺ 675.3912).

Anal. calcd. for **Pp8 (21H,23H-Porphine-2,18-dipropanoic acid, 7,12-diethenyl-3,8,13,17-tetramethyl-, 2,18-diocyl ester)**. Yield 81%. ¹H NMR (CDCl₃, 300 MHz): δ, ppm -3.53 (br s, 2H, H-21 and H-23); 0.65 and 0.67 ((t, 3H, $J = 7.5$ Hz) and (t, 3H, $J = 7.5$ Hz), H-13¹¹ and H-17¹¹); 1.15–1.42 (m, 20H, Hs-13⁶-13¹⁰ and Hs-17⁶-17¹⁰); 1.65 (m, 4H, $J = 7.0$ Hz, H-13⁵ and H-17⁵); 3.25 (t, 4H, $J = 7.5$ Hz, H-13² and H-17²); 3.60; 3.66; and 3.67 (3s, 6H, 3H and 3H, H-2, H-7, H-12 and H-18); 3.97 and 3.98 (two overlapping t, 4H, $J = 7.0$ Hz, H-13⁴ and H-17⁴); 4.39 (t, 4H, $J = 7.0$ Hz, H-13¹ and H-17¹); 6.16 (d, 2H, $J = 11.5$ Hz, H-3^{2α} and H-8^{2α}); 6.35 (d, 2H, $J = 17.0$ Hz, H-3^{2β} and H-8^{2β}); 8.24 (dd, 2H, $J = 17.0$ and 11.5 Hz, H-3¹ and H-8¹) 10.01, 10.11 and 10.13 (3s, 2H, 1H and 1H, H-5, H-10, H-15 and H-20). ESI-MS-TOF: m/z 787.5157 calcd. for C₅₀H₆₇N₄O₄⁺ (calcd. for [M + H]⁺ 787.5161).

Anal. calcd. for **Pp12 (21H,23H-Porphine-2,18-dipropanoic acid, 7,12-diethenyl-3,8,13,17-tetramethyl-, 2,18-didodecyl ester)**. Yield 84%. ¹H NMR (CDCl₃, 300 MHz): δ, ppm -3.70 (br s, 2H, H-21 and H-23); 0.82 (t, 6H, $J = 7.0$ Hz, H-13¹⁵ and H-17¹⁵); 0.84–1.31 (m, 40H, H-alkyl); 1.38 (m, 4H, $J = 7.0$ Hz, H-13⁵ and H-17⁵) 3.24 (t, 4H, $J = 7.0$ Hz, H-13² and H-17²); 3.57; 3.62 and 3.63 (3s,

6H, 3H and 3H, H-2, H-7, H-12 and H-18); 4.03 (t, 4H, $J = 7.0$ Hz, H-13⁴ and H-17⁴); 4.36 (t, 4H, $J = 7.5$ Hz, H-13¹ and H-17¹); 6.15 (d, 2H, $J = 11.5$ Hz, H-3^{2α} and H-8^{2α}); 6.33 (d, 2H, $J = 17.0$ Hz, H-3^{2β} and H-8^{2β}); 8.20 (dd, 2H, $J = 17.0$ and 11.5 Hz, H-3¹ and H-8¹) 9.94, 9.96, 10.05 and 10.06 (4s, 4H, H-5, H-10, H-15 and H-20). ESI-MS-TOF: m/z 899.6409 calcd. for C₅₈H₈₃N₄O₄⁺ (calcd. for [M + H]⁺ 899.6403).

Spectroscopic and photophysical studies

The porphyrin solutions analyzed in this work were obtained from a 1.0×10^{-3} M stock solution in dimethylsulfoxide. The spectra of electronic absorption in the ultraviolet-visible region and fluorescence emission of porphyrins were obtained in the concentration of 5.0×10^{-6} M in different solvents (ethanol-EtOH; methanol-MeOH; tetrahydrofuran-THF; acetonitrile-ACN; dimethylformamide-DMF; dimethylsulfoxide-DMSO) and the respective surfactants (Triton X-100, SDS, CTAB). Moreover, the measurements involving the surfactants were obtained at different pH values. The absorption spectra were obtained using a UV-vis spectrophotometer (Lambda 25, Perkin Elmer) and the fluorescence spectra were obtained using a fluorescence spectrophotometer (LS55, Perkin Elmer). The excitation wavelength used for measurements of fluorescence was obtained from the length of maximum absorption in the electronic absorption measurements in the UV-vis. The fluorescence quantum yield (Φ_F) was determined in the solvents, making use of anthracene in ethanol as standard solution, $\Phi_F = 0.27$ [42]. All measurements were obtained at 20 °C.

Measurements of fluorescence decay intensity were obtained by the method Single Photon Counting. The laser pulses were obtained with a titanium-sapphire laser (Tsunami 3950, Spectra Physics), which was pumped by a solid-state laser (Millenia Xs, Spectra Physics). The light output of this laser has an integrated power in the range between 6.0 and 10.0 W. The frequency of the pulses generated by the Tsunami is adjusted by a Pulse Picker (3986, Spectra Physics), which generates laser pulses in the range between 840 and 1000 nm. A pulse selector controls the repetition frequency of the pulses. The desired laser radiation can be obtained by a generator of second and third harmonics. At the specific case of porphyrins, the second harmonic with excitation at 414 nm was used in the measurements. The laser pulses of excitation are correlated temporally with pulses of fluorescence emitted by the sample, being the data detected and collected by a spectrometer (Edinburgh Instruments).

The spectrometer has a sample holder thermostated by a circulating water bath. The anisotropy decay was measured using a compensator (Babinet-Soleil BSC, Halbo Optics) in the excitation beam and a polarizer (P920, Edinburgh Instruments) of prism Glan-Thompson in the beam emission. The fluorescence lifetimes of

the porphyrins were determined in different solvents (DMSO, EtOH and ACN) and in micro-heterogeneous systems (in the presence of surfactants).

Heterogeneous media were generated by the dissolution of porphyrins in solutions of surfactants with time of stirring of 15 min. The concentration of surfactant was 40.0×10^{-3} M, which corresponds to a value higher than the critical micelle concentration (CMC). This indicates also that the micelle is the micro-heterogeneous structure prevalent in this chemical system. The final concentration of porphyrins in the micellar media was 1.0×10^{-5} M. To measure the time-resolved fluorescence, the wavelengths of excitation and emission were 414 nm and 630 nm, respectively. All measurements were performed at 20 °C.

CONCLUSION

Marked differences were observed in the photophysical properties (absorption, emission, quantum yield, fluorescence lifetime and orientational time) between the porphyrin derivatives and the different chemical environments. The porphyrin derivatives have shown a decrease in quantum yield and fluorescence lifetime in more polar solvents. Constants of fluorescence decay, which were calculated from the absorption spectra, are higher than those calculated from the lifetime data obtained experimentally. However, both data show similar tendency with respect to the solvent polarity. The size of the hydrophobic chains of the porphyrin derivatives has a significant influence in their interactions with surfactants, especially with respect to sodium dodecyl sulfate. It was also observed a large increase of Φ_F generated by Pp12 in solvents with lower polarity (DMF and THF), when compared to other solvents whose Φ_F data were close to zero. The incorporation of porphyrins in micellar systems was confirmed by fluorescence decay through a simple exponential curve for all porphyrins. This model is in agreement with data in the literature, where the porphyrin is confined in a region near the micellar surface. No difference was noticed for the rotational time as the alkyl chains of porphyrin become longer, which indicates that the position of the porphyrin in the micelles was not influenced by the presence of long nonpolar chains. Protoporphyrin-IX derivatives can be considered as a model of hydrophobic molecule with a high affinity for non-ionic surfactants. This increased affinity can be explained by the significant presence of Van der Waals interactions, which influence directly the properties of fluorescence and allow more effective stabilization of porphyrins in neutral micelles when compared to its stability in micelles consisting of ionic surfactants. In this study the emitting species were identified as well as its photophysical behavior as potential photosensitizer in different chemical environments. These information are fundamental to develop the most suitable prototype for application in PDT.

Acknowledgements

The authors are grateful to Prof. Dr. Amando Siuiti Ito by the use of the equipment to measure the lifetime with temporal resolution and by the financial support of Chamada Pública MCT/CNPq/MEC/CAPES — Ação transversal n° 06/2011 — Casadinho/Procad — Process n° 552197/2011-4. Hueder Paulo Moisés de Oliveira thanks to CNPq — Process 474019/2012-8 and 479655/2008-1. Maurício da Silva Baptista thanks to FAPESP — Process 2012/50680-5.

Supporting information

Figures S1–S6 are given in the supplementary material. This material is available free of charge via the Internet at <http://www.worldscinet.com/jpp/jpp.shtml>.

REFERENCES

1. Sternberg ED, Dolphin C and Brückner C. *Tetrahedron* 1998; **54**: 4151–4202.
2. Pradeepa SM, Naik HSB, Kumar BV, Priyadarsini KI, Barik A and Naik TR. *Spectrochim. Acta, A* 2013; **101**: 132–139.
3. Berg K, Anholt H, Moan J, Rgnnestad A and Rimington C. *J. Photochem. Photobiol., B* 1993; **20**: 37–45.
4. Zheng W, Shan N, Yu L and Wang X. *Dyes Pigments* 2008; **77**: 153–157.
5. Strauss WSL, Gschwend MH, Sailer R, Schneckenburger H, Steiner R and Ruck A. *J. Photochem. Photobiol., B* 1995; **28**: 155–161.
6. Macdonald IJ and Dougherty TJ. *J. Porphyrins Phthalocyanines* 2001; **5**: 105–129.
7. Nantes IL, Durán N, Pinto SMS, Silva FB, Souza JS, Isoda N, Luz RAS, Oliveira TG and Fernandes VG. *J. Braz. Chem. Soc.* 2011; **22**: 1621–1633.
8. Dougherty TJ, Gomer CJ, Henderson BW, Kessel GJD, Korbelik M, Moan J and Peng Q. *J. Natl. Cancer I.* 1998; **90**: 889–905.
9. Bonnett R. *Chem. Soc. Rev.* 1995; **24**: 19–33.
10. Detty MR, Gibson SL and Wagner SJ. *J. Med. Chem.* 2004; **47**: 3897–3915.
11. Santiago PS, Neto DS, Gandini SMC and Tabak M. *Colloids Surf., B* 2008; **65**: 247–256.
12. Dougherty TJ. *J. Clin. Laser Med. Sur.* 2002; **20**: 3–7.
13. Chwilkowska A, Saczko J, Modrzycka T, Marcinkowska A, Malarska A, Bielewicz J, Patalas D and Banas T. *Acta Biochim. Polonica* 2003; **50**: 509–513.
14. Marchal S, Fadloun A, Maugain E, D'Hallewin MA, Guillemin F and Bezdetnaya L. *Biochem. Pharmacol.* 2005; **69**: 1167–1176.
15. Andrade SM, Teixeira R, Costa SMB and Sobral AJFN. *Biophys. Chem.* 2008; **133**: 1–10.

16. Detty MR, Gibson SL and Wagner SJ. *J. Med. Chem.* 2004; **47**: 3897–3915.
17. Kadish KM, Maiya GB, Araullo C and Guillard R. *Inorg. Chem.* 1989; **28**: 2725–2731.
18. Phukan S, Mishra B, Shekar KPC, Kumar A, Kumar D and Mitra S. *J. Lum.* 2013; **134**: 232–239.
19. Techen A, Hille C, Dosche C and Kumke MU. *J. Colloid Interf. Sci.* 2012; **377**: 251–261.
20. Visser AJWG. *Curr. Opin. Colloid Interface Sci.* 1997; **2**: 27–36.
21. Valicsek Z and Horváth O. *Microchem. J.* 2013; **107**: 47–62.
22. Schweitzer-Stenner R. *J. Porphyrins Phthalocyanines* 2011; **15**: 312–337.
23. Gurinovich GP, Sevchenko AN and Solov'ev KN. *Sov. Phys. Uspekhi* 1963; **6**: 67–105.
24. Calzavara-Pinton PG, Venturini M and Sala R. *J. Eur. Acad. Dermatol.* 2007; **21**: 293–302.
25. Reichard C. *Chem. Rev.* 1994; **94**: 2319–2358.
26. Smallwood IM. *Handbook of Organic Solvent Properties*, John Wiley & Sons Inc.: New York, 1996.
27. Masoud MS, Ali AE, Shaker MA and Ghani MA. *Spectrochim. Acta, A* 2005; **61**: 3102–3107.
28. He X, Zhou Y, Wang L, Li T, Zhang M and Shen T. *Dyes Pigm.* 1998; **39**: 173–182.
29. Bojinov V and Panova I. *J. U. Chem. Techn. Met.* 2006; **41**: 277–284.
30. Glusko CA, Previtali CM, Vera DMA, Chesta CA and Montejano HA. *Dyes Pigm.* 2011; **90**: 28–35.
31. Naik LR, Naik AB and Pal H. *J. Photochem. Photobiol., A* 2009; **204**: 161–167.
32. de Oliveira HPM, Junior AM, Legendre AO and Gehlen MH. *Quim. Nova* 2003; **26**: 564–569.
33. Kubinyi M, Grofcsik A, Kárpáti T and Jones WJ. *Chemical Physics* 2006; **322**: 247–253.
34. Donovalová J, Cigáň M, Stankovičová H, Gašpar J, Danko M, Gáplovský A and Hrdlovič P. *Molecules* 2012; **17**: 3259–3276.
35. Yamaguchi Y, Matsubara Y, Ochi T, Wakamiya T and Yoshida ZY. *J. Am. Chem. Soc.* 2008; **130**: 13867–13869.
36. Galinier F, Bertorelle F and Fery-Forgues S. *C. R. Acad. Sci. Ser. II Fascicule C-Chim.* 2001; **4**: 941–950.
37. Inamura I and Uchida K. *Bull. Chem. Soc. Jpn.* 1991; **64**: 2005–2007.
38. Scolaro LM, Castriciano M, Romeo A, Patanè S, Cefalì E and Allegrini M. *J. Phys. Chem. B* 2002; **106**: 2453–2459.
39. Maiti NC, Mazumdar S and Periasamy N. *J. Phys. Chem.* 1995; **99**: 10708–10715.
40. Uchoa AF, Oliveira CS and Baptista MS. *J. Porphyrins Phthalocyanines* 2010; **14**: 832–845.
41. Uchoa AF, De Oliveira KT, Baptista MS, Bortoluzzi AJ, Iamamoto Y and Serra O A. *J. Org. Chem.* 2011; **76**: 8824–8832.
42. Lakowicz JR. *Principles of Fluorescence Spectroscopy* (2nd ed), Kluwer Academic: New York, 1999.